

1 New viruses of *Cladosporium* sp. expand considerably the taxonomic structure
2 of *Gammartivirus* genus
3
4

5 Augustine Jaccard, Nathalie Dubuis, Isabelle Kellenberger, Justine Brodard, Sylvain Schnee,
6 Katia Gindro and Olivier Schumpp
7

8 Department of Plant protection, Agroscope, Nyon, Switzerland
9

10 **Abstract**

11 Despite the fact that *Cladosporium* sp. are ubiquitous fungi, their viromes have been little
12 studied. By analysing a collection of *Cladosporium* fungi, two new partitiviruses named
13 *Cladosporium cladosporioides* partivirus 1 (CcPV1) and *Cladosporium cladosporioides*
14 partivirus 2 (CcPV2) co-infecting a strain of *Cladosporium cladosporioides* were identified.
15 Their complete genome consists in two monocistronic dsRNA segments (RNA1 and RNA2)
16 with a high percentage of pairwise identity on 5' and 3' end. The RNA dependant RNA
17 polymerase (RdRp) of both viruses and the capsid protein (CP) of CcPV1 display the classic
18 characteristics required for their assignment to the *Gammartivirus* genus. In contrast,
19 CcPV2 RNA2 encodes for a 41 KDa CP that is unusually small with a low percentage of amino
20 acid identity as compared to CPs of other viruses classified in this genus. This sequence was
21 used to annotate fifteen similar viral sequences with unconfirmed function. The phylogeny of
22 the CP was highly consistent with the phylogeny of their corresponding RdRp, supporting the
23 organization of gammartiviruses into three distinct clades despite stretching the current
24 demarcation criteria.

25 **Introduction**

26 A large number of different microorganisms, such as filamentous fungi, yeasts, viruses or
27 bacteria, naturally colonise the vine [1, 2]. These organisms, collectively known as the plant
28 microbiome, develop interactions with each other and with their hosts, all contributing to the
29 functioning and evolution of a discrete ecological entity referred to as the holobiont [3–7].
30 These interactions can influence plant growth, response to pathogens, metabolite productions
31 and adaptation to environmental changes [1, 8].

32 The holobiont protagonists combine different levels of interaction and the presence of
33 mycoviruses infecting endophytes may sometimes favour the development of the host plant
34 with potentially interesting agronomical consequences. Seminal work has demonstrated the
35 role of the mycovirus *Cryphonectria hypovirus 1* in reducing the virulence of *Cryphonectria*
36 *parasitica*, the fungus responsible for chestnut blight fungus [9, 10]. A more recent study
37 showed that the mycovirus *Sclerotinia sclerotiorum* hypovirulence-associated DNA virus 1
38 down-regulates pathogenicity factors of its fungal host, *Sclerotinia sclerotiorum*, resulting in a

39 reduction in fungal virulence and conferring it beneficial endophytic properties that stimulates
40 plant growth and response to stress [11]. Hence, mycoviruses appear as putative solutions for
41 plant protection and especially for vine cultivation that requires quantities of phytosanitary
42 products with a strong impact on natural ecosystems. These mycoviruses are particularly
43 abundant in the grapevine, where their great diversity has been revealed by high-throughput
44 sequencing analyses [12–14].

45 *Cladosporium*, one of the largest genera of dematiaceous fungi present in the environment, is
46 also dominant as grapevine endophyte [15–17]. Its presence on leaves and berries increases
47 progressively with the growing season [18] and late harvesting can favour the development of
48 *Cladosporium* rot on the berries (*C. cladosporioides* and *C. herbarum*) which affects wine
49 quality [19]. We analysed the prevalence and genome of viruses of this ubiquitous fungal
50 species to understand better their role and the possible exchanges of viruses within vine fungal
51 communities.

52 An approach based on the extraction of virion-associated nucleic acids (VANA), originally
53 adapted for plant viruses, has proved highly effective on fungal mycelium. Four genomic
54 segments forming two *Partitivirus* coexisting in *Cladosporium* sp. were identified and
55 characterized.

56 This work enabled us to assign a structural function to 15 hypothetical viral proteins that form
57 a distinct clade in the genus *Gammapartitivirus*. It includes viruses with a novel capsid protein
58 sequence showing very little similarities to the capsid protein sequences of any other
59 *Gammapartitivirus*.

60 **Material and method**

61

62 **Fungal isolates**

63 The fungal community was isolated from sap bleedings collected on an Agroscope
64 experimental plot at Leytron (VS, Switzerland). The sap was collected in 50mL brown glass
65 bottles. Bottles were sterilized with ethanol, sealed with parafoil and left for 2 weeks during the
66 bleeding season. 100µL of sap sample diluted hundred times with sterile water were plated on
67 Potatoes Dextrose Agar with aureomycin 12 mg.L⁻¹ (PDAa). Fungi were isolated by subculture
68 of emerging mycelium on PDA petri dishes. In total, 249 fungal isolates were cultured from the
69 grapevine bleeding sap of 41 vinestocks. A visual classification based on the morphology of
70 the colonies revealed a predominance of *Cladosporium* and *Aureobasidium* as previously
71 reported on grapevines [16, 18]. To avoid the analysis of individuals from the same lineage,
72 only one isolate of each genus was selected per plant. Their identity was confirmed by ITS
73 sequencing of a representative isolate using ITS1F/ITS4 primer as previously described [20].

74 Twenty-two *Aureobasidium* isolates, 14 *Cladosporium* isolates and 12 isolates representing
75 the diversity of colony morphotypes were selected for virus screening.

76 Following the identification of a virus in a *Cladosporium* strain, 12 *Cladosporium* isolates
77 present in Agroscope's fungal collection (www.mycoscope.ch/) were further screened by RT-
78 PCR for the presence of this virus.

79

80 **Semi-purification of virus particles**

81 The particle purification was performed according to a previously-described protocol with some
82 modifications [21]. Briefly, 15-30 g of fresh mycelium from Potatoes Dextrose Agar culture were
83 ground into small powder using liquid nitrogen and a mixer (Sovall Omni Mixer 17150
84 Homogenizer). The powder was supplemented with 6 vol of extraction buffer (0.5 M Tris, pH
85 8.2, 5% v/v Triton, 4% v/v Polyclar AT, 0.5% w/v bentonite, 0.2% v/v β -mercaptoethanol) and
86 stirred on ice. After 20 min of homogenisation, the suspension was filtered through a double
87 layer of cotton cloth. About 120 ml of filtrate was centrifuged at 4,000 rpm for 20 min. The
88 supernatant was then collected and placed on 5 ml of 20% sucrose cushion (diluted in 0.1 M
89 Tris, pH 8.2) followed by centrifugation at 40,000 rpm using a Beckman Coulter SW32Ti rotor
90 for 1.5 h. The resulting pellet was incubated overnight at 4°C in 1 ml of suspension buffer (0.02
91 M Tris, pH 7.0, 0.001 M $MgCl_2$). Enrichment in viral particles was verified by electron
92 microscopy using 3 μ l of particles as previously described [22], using the Tecnai G2 Spirit
93 microscope (FEI, Eindhoven).

94

95 **RNA extraction**

96 Total RNA extraction from fungal field isolates sub-cultured on agar plates was carried out
97 according to Akbergenov et al. (2006) with the following modifications: 0.5 cm² square of
98 mycelium (50-100 mg) was cut from the edge of the plate with a scalpel, and placed in a 1,5mL
99 Eppendorf tube with three 3 mm glass beads and frozen in liquid nitrogen. The grinding was
100 carried out by shaking the tubes in a TissueLyser (Qiagen) for 60 seconds at 30 Hz. If
101 necessary, the operation was repeated once after incubation in liquid nitrogen. 1 ml of
102 extraction buffer (6.5 M Guanidine hydrochloride; 100mM tris HCL pH=8; 100 mM β -
103 mercaptoethanol) was added to the tube and mixed. The samples were incubated at room
104 temperature for 10 minutes and then centrifuged for 10 minutes at 12000 rpm at 4 °C. The
105 supernatant was transferred to a 2 ml Eppendorf tube. After the addition of 0.5 mL of Trizol
106 (Invitrogen) reagent and 0.2 mL of Chloroform, tubes were centrifuged 10 minutes at 12 000
107 rpm. The upper phase was transferred to a RNase-free 50 mL polypropylene Beckman Bottles,
108 supplemented with an equivalent volume of isopropanol, and incubated on ice for 30 minutes.
109 The tube was centrifuged for 20 minutes at 12,000 rpm at 4°C. The pellet was washed in 70%
110 ethanol, dried at room temperature, resuspended in 30 μ l H₂O and stored at -80°C.

111
112 VANA from the Agroscope's fungal collection isolate *C. cladosporioides* AGS-1338 grown on
113 PDA medium were extracted according to the protocol initially adapted for plant virus described
114 in [24, 25]. Briefly, 200 μ L of semi-purified particles described above were treated with 1 μ L of
115 DNase and 1 μ L of RNase (Euromedex) for 90 minutes at 37°C to remove non-encapsulated
116 RNA and DNA as described previously by Maclot et al. (2021). 400 μ L of lysis buffer from the
117 RNeasy plant mini kit (Qiagen) and 60 μ L of N-Laurylsarcosine sodium salt solution 30% were
118 added and mixed and 500 μ L of the solution were loaded on a QIAshredder spin column and
119 further processed according to manufacturer's recommendation.

120

121 **Library preparation, sequencing and bioinformatic analyses**

122 Total RNA extracted from 22 isolates from *Aureobasidium* sp., 14 isolates from *Cladosporium*
123 sp. and 12 isolates representing other fungal species were pooled with equal quantity and
124 treated for DNase with the RNeasy mini prep kit (Qiagen). RNA quality was controlled with a
125 BioAnalyzer (Agilent Technology). A final extract of approximately 2.6 μ g was used for the
126 preparation of the cDNA library. Small RNA library preparation was performed with TruSeq
127 small RNA kit, and mRNA with TruSeq Stranded mRNA kit. cDNA for mRNA and small RNA
128 were sequenced using an Illumina NextSeq High library preparation kit and sequenced on an
129 Illumina NextSeq 550 System (Illumina, USA) in paired-end 2x75 nt reads by Fasteris
130 (Genesupport, Switzerland). Raw reads were trimmed with BBDuk 37.64 plugin and
131 assembled using SPAdes plugin in Geneious Prime 2019.0.4 [27, 28].

132 Synthesis of the cDNA and tagged-library preparation from VANA was performed as described
133 by Candresse et al. (2014) using TruSeq™ DNA Nano kit. Library quality was controlled using
134 a Bioanalyzer 2100 and sequenced at Fasteris (Genesupport, Switzerland) on Miseq nano kit
135 version 2 (Illumina, USA) in 1x50+8+8 cycles. Reads trimming was carried out using BBDuk
136 38.37 plugin from Geneious Prime 2020.0.4 (Biomatters, Auckland), and *de novo* assembly
137 was performed using parameters of the high sensitivity mode from Geneious assembler.

138

139 **Reconstruction of whole genomic sequences and annotation**

140 Contigs were selected and annotated using blastn on a "in-house" mycovirus database
141 including viral genus of previously described mycoviruses, prepared from refseq sequences
142 present in NCBI (01.05.2020). Reads were mapped to reference sequences identified by blast
143 and primers were designed on reads stacks to confirm the sequence of each contig by Sanger
144 sequencing and reconstruct the full genomes by RACE PCR (**Table S1**). AMV reverse
145 transcriptase (Promega, Switzerland) and GoTaq polymerase (Promega, Switzerland) were
146 used for a one-step protocol. RT-PCR cycling conditions were 45 minutes at 48°, followed by
147 2 minutes at 94°C, then 35 cycles of 45 seconds at 94°C, 40 seconds at 55°C and 1,5 minutes

148 at 72°C, ended by 10 minutes at 72 °C. A denaturing step was applied according to Asamizu
149 et al. [29] before using the SMARTer RACE 5'/3' Kit (5' section only) according to
150 manufacturer's recommendations. Amplified RACE and RT-PCR products were cloned in
151 pGEM-T, sequenced and assembled using Geneious assembler with highest sensitivity
152 parameters. Reads were mapped on the assembled sequences to control the assembly. An
153 extra stretch of 7 nucleotides (ACATGGG) detected in all RACE sequences but not described
154 in the kit specification was removed.

155 The annotation of the selected contigs was verified by online blastn and blastx analysis. The
156 presence and size of an Open Reading Frame (ORF) was predicted for each segment by ORF
157 finder (ncbi.nlm.nih.gov/orffinder).

158
159

160 **Viral particles characterisation**

161 Virus particles were concentrated with a 10-40% sucrose gradient prepared with a Buchler
162 gradient maker (Buchler Instruments Inc., Fort Lee, NJ, USA) with 17.5 mL of 10% (v/v) and
163 17.5 mL of 40% (v/v) sucrose in the suspension buffer (0.02 M Tris, pH 7.0, 0.001 M MgCl₂).
164 One milliliter of virus particles was overlaid on the sucrose gradient and ultracentrifuged for 2.5
165 hours at 30,000 rpm at 4 °C using a Beckman Coulter SW32Ti rotor. After centrifugation,
166 fractions of 1.8 mL from top to bottom were collected and numbered from #1 to #20. Groups
167 of three fractions were pooled, diluted in 40 mL of suspension buffer and centrifuged 2.5 h at
168 40'000 rpm. The pellet was suspended in 200 µL suspension buffer. Fraction groups #10 to
169 #12, #13 to #15 and #16 to #18 were visualized by TEM. Particles from fraction #13 to #15
170 were used to measure the diameter of particles with ImageJ [30]. The calculation of the mean,
171 standard deviation and the mean comparison with a student t.test was performed in R.

172

173 **LC-MS/MS**

174 The semi-purified particles were loaded onto a 12% (v/v) sodium dodecyl sulfate-
175 polyacrylamide gel electrophoresis (SDS-PAGE) gel. A 100 kDa size marker was used for size
176 estimation (Biorad, low range standards). After electrophoresis, the gel was stained with
177 Coomassie brilliant blue R250. The resulting band of the expected size of the putative capsid
178 of CcPV1 and CcPv2 were excised and subjected to mass spectrometry coupled to liquid
179 chromatography (LC-MS/MS) analysis at the Centre for Integrative Genomics (University of
180 Lausanne, Switzerland) for determination of protein sequence.

181

182 **Annotation and phylogenetic analysis**

183 The protein sequences encoding for RdRp and CP identified in this work were aligned with the
184 protein sequences of members of the family *Partitiviridae* available from ICTV website and
185 other members of newly described zeta and epsilon genus [31, 32] (**Table S2**). The Human

186 picobirnavirus strain Hy005102 reference sequence was used as an outgroup of the RdRp
187 tree. Alignment was performed using MUSCLE version 3.8.425 implemented in Geneious
188 Prime 2020.0.4 with standard parameters [33]. The resulting alignment quality was verified
189 manually and zones with alignment ambiguities were excluded for tree and distance matrix
190 calculation. The phylogenetic tree was conducted with IQ-tree, using the optimised model for
191 maximum likelihood method [34, 35]. Branching support was obtain with 1000 bootstrap with
192 the ultrafast method from IQ-Tree [36]. The phylogenetic trees were curated on iTol [37].
193 Research for protein domains was done with CDsearch of NCBI in the pfam database [38] and
194 annotation of the sequence was done with ORF finder from NCBI to identify the proper coding
195 region of the sequence.

196

197 **Results**

198 **Virus identification**

199 Despite the elevated number of reads and contigs generated by Illumina sequencing of pooled
200 fungal RNA prepared from 48 isolates collected in Leytron, only one viral contig of 123 bp could
201 be confirmed by RT-PCR. This contig was identified in the *C.ramotenellum* strain AGS-Cb3.2
202 only. A fragment of 101 bp was amplified with the primer set 10/89 and shared 93% identity
203 with the NCBI sequence MN034127 reconstructed from a soil metagenome study annotated
204 as a *Partitiviridae* sp. [39]. In the absence of reverse transcription, no amplification was
205 observed confirming the viral replicative nature of the fragment.

206 New primers (193/1035) designed on the sequence MN034127 enabled the amplification of a
207 longer fragment of 1218 nucleotides that lead to the complete genomic fragment reconstruction
208 by RACE-PCR from AGS-Cb3.2. Read mapping on this complete sequence showed that only
209 15 reads covering 13% of the sequence mapped on this sequence with 100% identity. As low
210 viral titer suggested by the weak read coverage of the sequence could be due to active
211 silencing activity, a second Illumina sequencing targeting siRNAs from the same mixed extract
212 was performed (**Fig. S1A**). Only one read of 28 bp from sRNAs between 15 and 30 nt in size
213 was associated with this fragment by mapping with Bowtie 2.

214 The infected AGS-Cb3.2 strain could not be maintained.

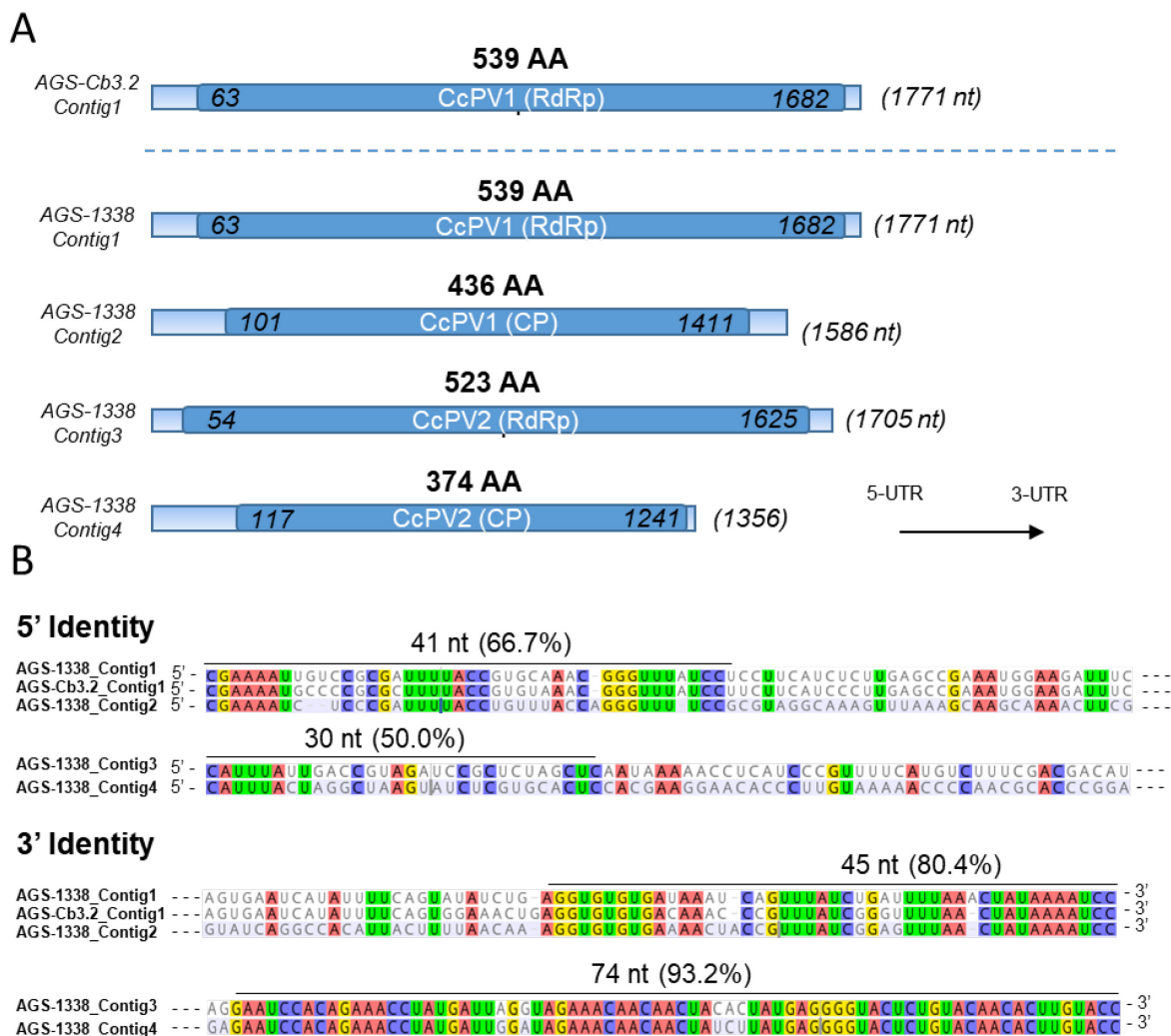
215 Twelve *Cladosporium* isolates maintained in the Agroscope fungal isolate collection
216 (<https://mycoscope.bcis.ch/>) were then screened by RT-PCR using the primer 10/89. The *C.*
217 *cladosporioides* strain AGS-1338 isolated from a vine stock of Chasselas in 2010 in Perroy
218 (VD, Switzerland) produced a band corresponding to the expected viral fragment size, and the
219 viral sequence was confirmed with sanger sequencing of the purified band (**Fig. S2B**). The
220 identity of the fungal isolate was confirmed by sequencing and blastn analysis of the ITS
221 sequence.

222

223 Mycovirus genomes reconstruction

224 A third Illumina sequencing was performed using the *C. cladosporioides* isolate AGS-1338 to
 225 reconstruct the complete genome of the virus previously detected in AGS-Cb3.2, especially
 226 the second genomic fragment of this virus whose affiliation to the *Partitiviridae* family required
 227 a bisegmented genome [40]. The sequencing strategy was based on a protocol initially
 228 adapted for plant virus using VANA instead of total RNA extracts [24]. From the sequencing
 229 data, four contigs were significantly longer with sizes of 1629, 1953, 1980 and 2139 bp (**Fig.**
 230 **S1B**). RT-PCR with primers designed on these four contigs confirmed their presence in the
 231 strain AGS-1338. The exact 5' and 3' ends of each fragment were determined with RACE-
 232 PCR, and the full genome sequences were confirmed by Sanger sequencing. Final sequences
 233 were smaller than those obtained by the bioinformatics analysis of Illumina reads with sizes of
 234 1356, 1586, 1771 and 1705 nucleotides (**Fig. 1A**). These sequences were covered by 33.3%,
 235 21 %, 12.4% and 27.4 % of the total reads obtained by Illumina sequencing, respectively (**Fig.**
 236 **S1**).

237



238

239 **Fig. 1: characteristic of the sequences of CcPV1 and CcPV2 detected in strain *C. cladosporioides* AGS-1338 and**
240 ***C. ramotenellum* Cb3.2.** A] Viral contigs. Coding sequences are highlighted in dark blue and the 5'- and 3'-UTRs
241 sequences in light blue. Nucleic acid position of the start and end of the ORF is indicated. The size of the full
242 nucleic sequence is in brackets. B] Alignment of the 5'- and 3'-UTRs of the genomic segments present in isolates
243 AGS-1338 and AGS-Cb3.2. Nucleotides shared among the different sequences are highlighted and the percentage
244 of identity of the most conserved parts is indicated.

245
246 A blastn and blastx analysis of the four contigs identified two sequences coding for RdRp
247 (Contig1 and 3) one CP (Contig2) and a Hypothetical Protein (HP, Contig4, **Fig. 2**). The four
248 sequences did not have a poly-A tail and showed a GC content between 45.1% and 52.7%,
249 which corresponded to the average GC content values for dsRNA viruses in general including
250 *Partitiviridae* [41]. An RT-like super family conserved domain was detected on Contig1 and 3
251 using CDsearch. The same analysis performed on the sequence reconstructed from *C.*
252 *ramotenellum* strain AGS-Cb3.2 lead to the identification of a unique ORF encoding a RdRp
253 (Contig1-Cb3.2) (**Fig. 1A**).

254 All segments were more than 90% identical to one or more viral segments assigned to the
255 *Partitiviridae* family. *Partitiviridae* are multisegmented virus, composed of two segments
256 encoding for a RdRp (RNA1) and a CP (RNA2) [40]. This genomic organisation was confirmed
257 for all 4 sequences by the analysis of the fragment ends. Contig1-1338 and Contig2-1338
258 termini showed a high sequence identity on both 5' and 3' ends, thereby confirming these two
259 genomic fragments encoding for an RdRp (RNA1) and a CP (RNA2) were forming the
260 complete genome of a virus (**Fig. 1B**). Contig1 and 2 were covered with the approximate same
261 number of reads (**Fig. 2**).

262 The UTR of the Contig3-1338 and Contig4-1338 also showed high sequence identity: they
263 shared a common stretch of 6 identical nucleotides at the 5' end and a long stretch of 71
264 identical nucleotides at the 3' (**Fig. 1B**). Contig3-1338 encoded for a RdRp. As shown by
265 protein sequencing (see results below), the Contig4-1338 encoded for a so far undescribed
266 CP type. Contig3 and 4 were also covered with the approximate same number of reads (**Fig.**
267 **2**). Thus, we concluded that both fragments corresponded to the RNA1 and RNA2 of a second
268 virus infecting AGS-1338. These two viruses are close to viral sequences derived
269 from metagenomic work and are referred to as "associated" with the host species under study.
270 In view of our work and the ubiquitous nature of *Cladosporium*, which is also very common on
271 grapevines, we consider this assignment to be too uncertain. In contrast, in our work, both
272 viruses were identified from a *Cladosporium* isolate in pure culture identified by sequencing
273 and maintained in a collection. They were verified by full-length sequencing. For all these
274 reasons, we provisionally named these viruses *Cladosporium cladosporioides* partitivirus 1
275 and 2, respectively, and hereafter refer to them as CcPV1 and CcPV2.

A

Contigs	Contig length (nt)	Mapped reads	Protein function	Bests hit identification (blastx)	Accession number	Query cover (%)	Identity (%)	E.value
Contig1-1338	1771	2207	RdRp	Erysiphe necator associated partitivirus 3	QJW70322.1	91%	92%	0E+00
				Erysiphe necator associated partitivirus 2	QJW70318.1	91%	90%	0E+00
Contig2-1338	1586	2154	CP	Plasmopara viticola lesion associated Partitivirus 3	QHD64799.1	82%	100%	0E+00
				Erysiphe necator associated partitivirus 3	QJW70321.1	82%	86%	0E+00
Contig3-1338	1705	4857	RdRp	Plasmopara viticola lesion associated Partitivirus 4	QHD64807.1	90%	99%	0E+00
				Plasmopara viticola lesion associated Partitivirus 3	QHD64801.1	89%	77%	0E+00
Contig4-1338	1356	5908	HP	Plasmopara viticola lesion associated Partitivirus 4	QHD64811.1	82%	97%	0E+00
				Colletotrichum gloeosporioides partitivirus 1	QED88096.1	82%	66%	1E-173

B

ORF	Contig length (nt)	Mapped reads	Protein function	Bests hit identification (blastn)	Accession number	Query cover (%)	Identity (%)	E.value
Contig1-1338	1771	2207	RdRp	Plasmopara viticola lesion associated Partitivirus 10	MN556983.1	92%	94%	0E+00
				Partitiviridae sp.	MN035614.1	97%	91%	0E+00
Contig2-1338	1586	2154	CP	Plasmopara viticola lesion associated Partitivirus 3	MN556982.1	99%	98%	0E+00
				Erysiphe necator associated partitivirus 3	MN605495.1	97%	84%	0E+00
Contig3-1338	1705	4857	RdRp	Plasmopara viticola lesion associated Partitivirus 4	MN556990.1	98%	96%	0E+00
				Hangzhou partiti-like virus 1	OM514386.1	94%	73%	0E+00
Contig4-1338	1356	5908	HP	Plasmopara viticola lesion associated Partitivirus 4	MN556994.1	92%	95%	0E+00

Fig. 2: Blast annotation for the four viral segments identified in AGS-1338. A) Blastx annotation B) Blastn annotation.

276
277
278
279

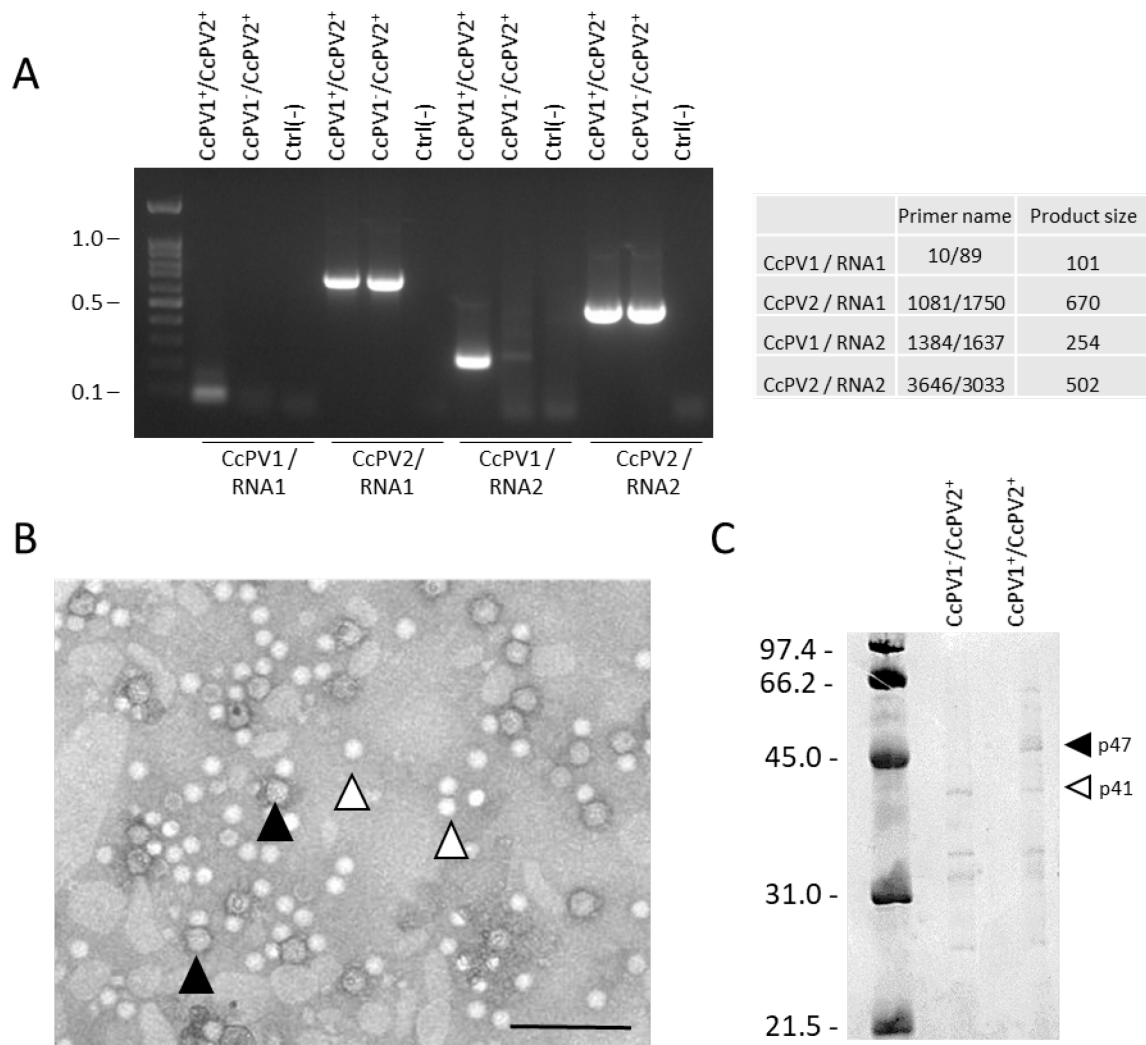
280

281 Virion characterisation and CP sequencing

282

283 Particles enrichment by ultra-centrifugation was verified by TEM. Two types of particles could
284 be observed (**Fig. 4B**). Large dense spherical particles of 36.2 ± 2.6 nm ($n = 25$) with a
285 contrasted outline distinguished from smaller bright spherical particles of 31.5 ± 2.4 nm ($n=25$)
286 in AGS-1338 hosting CcPV1 and CcPV2. A t-test supported the size difference (p .value = $4.3e$ -
287 **8; Table S3**).

288 Occasionally, the concentration of CcPV1 in some plate subcultures was lower. Drawn on this
289 finding, particle enrichments from two subcultures presenting high and low viral titre of the
290 CcPV1 but same titre of CcPV2 were prepared (**Fig. 4**). Protein separation performed on SDS-
291 PAGE showed two bands of about 47 and 41 kDa in the culture CcPV1⁺/CcPV2⁺ with high viral
292 titre of both viruses, corresponding to the calculated size of the ORF from RNA 2 of CcPV1
293 annotated as a CP and the calculated size of the ORF from RNA 2 of CcPV2 initially annotated
294 as HP, respectively (**Fig. 4B**). However, no band of 47 kDa was observed in the culture CcPV1-
295 /CcPV2⁺ with low viral titre of CcPV1, indicating that the missing p47 was indeed the CP of
296 CcPV1 (**Fig. 4C**). LC-MS/MS analysis yielded 34 unique peptides covering 83% CP of CcPV1
297 for the p47 protein while p41 protein sequencing yielded 26 unique peptides covering 79% of
298 the ORF of RNA 2 of CcPV2. These results demonstrated that the Contig4-1338 was a capsid
299 protein and was therefore referred to as CP of CcPV2.



300
 301 **Fig. 4: Analysis of the viral particles of *C. cladospiroides* AGS-1338.** A) RT-PCR of two sub-culture of AGS-1338.
 302 DNA ladder is 100 bp. B) TEM of semi-purified viral particles from *C. cladospiroides* AGS-1338. Black arrows
 303 designate larger viral particles. White arrow designates smaller viral particles. Scale bar represents 200nm. C)
 304 SDS-PAGE of semi-purified virus particles from CcPV1⁺/CcPV2⁺ and CcPV1⁻/CcPV2⁺ subcultures. Electrophoresis
 305 gel was stained with Coomassie blue.

306

307 **Phylogenetic analysis**

308 The two RdRp and CP sequences were aligned with protein sequences from representative
 309 members of the *Partitiviridae* family currently accepted by ICTV. The list was completed by
 310 viruses identified by blastx analysis of the CP for which RdRp was also available (**Table S2**).

311 The phylogenetic trees of both RdRps and CPs assigned CcPV1 and CcPV2 in the
 312 *Gammartivirus* genus. Both trees allowed the distinction of three subclades, named I, II
 313 and III, and showed a high degree of consistency for all but two viruses. *Plasmopara viticola*
 314 lesion associated Partitivirus 3 (PvIaPV3) had a RdRp grouped in clade III and a CP in clade
 315 II. *Ustilagoidea vires partitivirus* (UvPV) is an interesting case discussed in greater detail
 316 below. Its RdRp and its CP grouped in clade II, but this virus was associated with a third protein

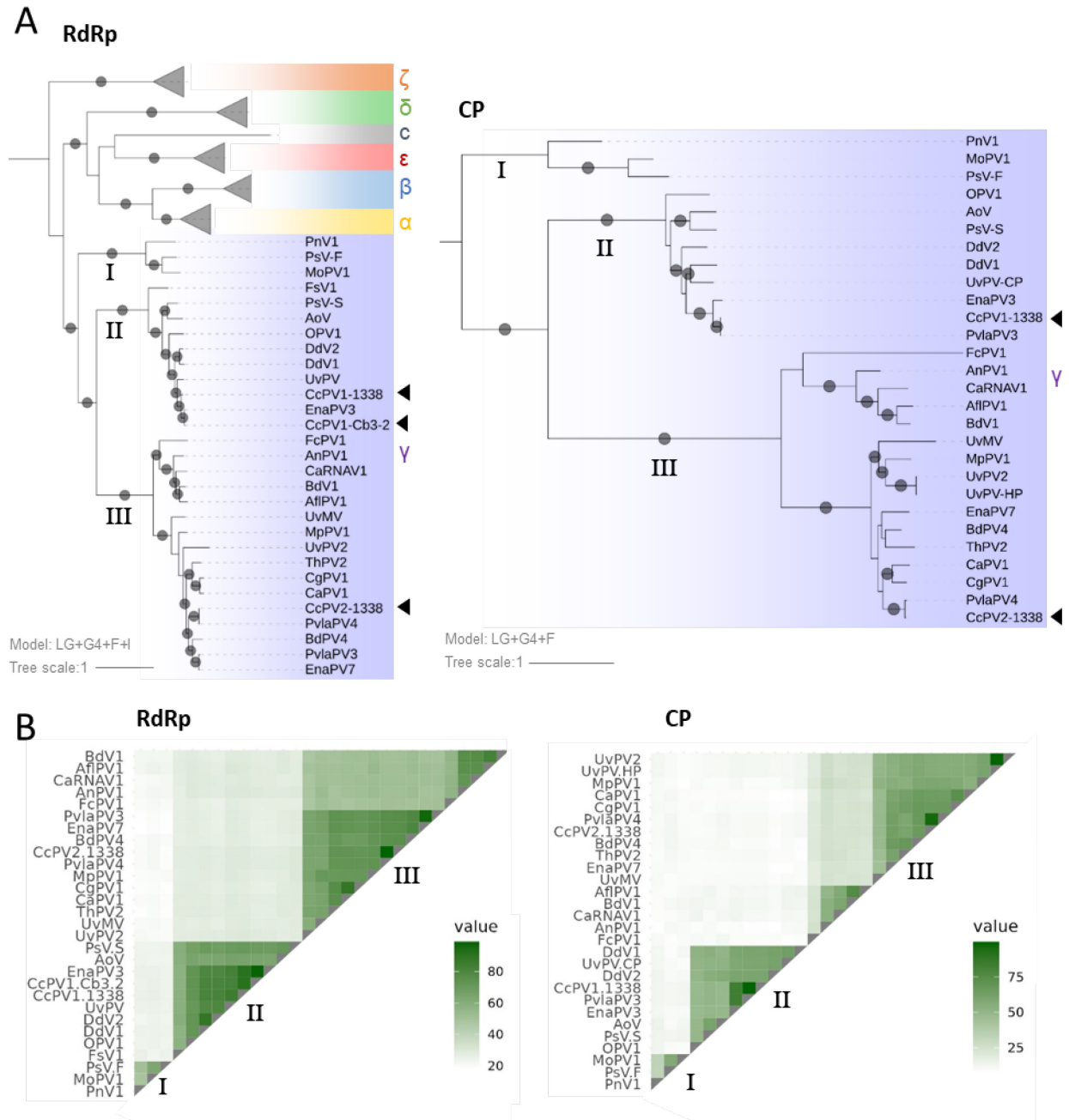
317 that clustered in clade III. In both trees, CcPV1 clustered in the sub-group II and CcPV2 in
318 clade III (**Fig. 3**).

319 The RdRp identified in AGS-Cb3.2 had over 92% amino acid identity with the CcPV1 RdRp.
320 Despite the lack of detection of a CP in AGS-Cb3.2, this high level of identity confirmed that
321 the viral sequence detected in AGS-Cb3.2 corresponded to another isolate of CcPV1, present
322 in another species of *Cladosporium*.

323 The RdRp of CcPV2 clustered in the Gamma genus with strong statistical support. However,
324 the percentage of amino acid sequence identity fall under the 24% threshold required to
325 delineate the *Partitiviridae* genus in pairwise comparisons with viruses of the clade I [40] (**Fig.**
326 **3B, Table S5**). The length of the RNA 2 encoding for the CP was 1356 nt that is 89 nt below
327 the 1445 to 1611 nt limits that are currently used to delimit the genus *Gammapartitivirus*.
328 Similarly, the length of the CP of CcPV2 (374 AA) and all viruses of group III were also well
329 below the limits of 413 – 443 AA also used to delimit the genus *Gammapartitivirus*.

330 In line with these results, the calculated weight of the CP of viruses from clade III were of 40-
331 42 KDa, close to the 41 KDa of the CP from CcPV2. This contrasted with the calculated weight
332 of 46-48 KDa of the CP of viruses currently accepted by ICTV clustering in clade I and II.
333 Finally, these results were also consistent with the particle sizes that could be measured:
334 *Penicillium stoloniferum* viruses S (PsV-S), having particles of about 35 nm in diameter [42]
335 was grouped in clade II with CcPV1 which had a particle size of 36.2 nm in diameter while
336 CcPV2 having particle size of 31.5 nm in diameter was assigned to clade III.

337



338
339
340
341
342
343
344
345
346
347
348
349
350
351
352

Fig. 3: Phylogenetic tree and pairwise identity matrix of RdRp and CP proteins. A) Bayesian Maximum likelihood phylogenetic tree. Bootstrap support values greater than 70% are indicated on the branches by a grey circle. The left tree was built with LG+F+I+G4 model with a selection of RdRp sequences of Partitiviridae family (Supplementary Table S2). HBPV was used as an outgroup. The tree on the right was built with LG+G4+F model with a selection of CP sequences of the *Gammartitivirus* family and blastx hits of CP-CcPV1 and -CcPV2. The tree was rooted according to the RdRp phylogenetic tree. B) Percentage of protein sequence identity with representative members of the *Gammartitivirus* genus and blastx hits of CP-CcPV1 and -CcPV2 for which RdRp was also available. The numerical values of the matrix are given in Tables S4 and S5.

353 Discussion

354 High-throughput sequencing analyses revealed the presence of numerous mycoviruses
355 representing a wide diversity of viral families in grapevine [12, 17]. Many examples of
356 mycoviruses are capable of altering the virulence of plant pathogenic fungi [43–45] and others
357 promote growth and/or sporulation [46–48]. However, despite some exceptions, some viral
358 families that are very common in filamentous fungi such as the *Partitiviridae* are less frequently
359 associated with a fungal phenotype [45, 49–51].

360 This apparent lack of phenotype raises questions about the role of these viruses in the
361 development cycle of their fungal host. In order to understand better virus-fungus interactions,
362 the aim of this study was to characterise the virome of fungal communities from grapevine
363 wood. *Cladosporium* sp. are known to be highly represented in grapevine fungal communities
364 and are also widespread in most ecological niches [17, 52]. This partly explains the large
365 number of *Cladosporium* virus sequences in the NCBI databases. Nevertheless, these
366 sequences are mainly derived from metagenomic work and form incomplete genomes in the
367 vast majority of cases. Consequently, only seven complete viral genomes from cultivated
368 isolates have been described to date [17, 53]. In this work, we carefully reconstructed and
369 characterised the complete genomes of CcPV1 and CcPV2, two new mycoviruses detected in
370 *Cladosporium* strains isolated from grapevine fungal communities. The presence of these
371 mycoviruses was evaluated in a collection of *Cladosporium* isolates. To our knowledge, this is
372 the first study specifically targeting *Cladosporium* isolates in pure cultures isolated from
373 grapevine fungal communities.

374 Illumina sequencing of 48 pooled RNA extract prepared from petri dish cultures proved to be
375 very insensitive: despite good RNA quality assessed by Nanodrop or Bioanalyzer and good
376 quality data set from Illumina sequencing, only one small contig corresponding to a viral RdRp
377 sequence of partitiviridae could be identified and confirmed by RT-PCR in a single fungal
378 isolate (Cb3.2) of the *C. ramotenellum* species. After reconstitution of the entire genomic
379 fragment corresponding to this contig, the read mapping produced very low coverage,
380 reflecting a low level of expression of the mycovirus in this strain under our culture conditions.
381 Compared to the study by Nerva et al. (2019), who detected mycoviruses in more than 15% of
382 isolates from the grapevine fungal community using similar amounts of RNA, but prepared
383 from liquid culture and with ribosomal depletion before library preparation, this result suggests
384 that total RNA from 50-100 mg petri dish cultures without viral RNA enrichment is not a
385 sufficiently sensitive method for viral genome reconstruction by high-throughput sequencing.
386 The strain *C. ramotenellum* Cb3.2 declined rapidly and could not be maintained in collections
387 or in liquid culture. Senescence phenomena are common in many fungal species [54, 55] and
388 in some cases the role of a mycovirus in reducing the life span of fungal species could be
389 demonstrated [56]. However, a stable strain of *C. cladosporioides* AGS-1338 maintained at

390 Changins for 12 years was also infected with this mycovirus, suggesting that this viral species
391 is not the cause of the decline of its fungal host. Thus, as for most *Partitiviridae* described so
392 far, this mycovirus does not appear to have a negative effect on the long-term survival of its
393 fungal host.

394 The sensitivity of mycovirus detection was drastically improved using a VANA enrichment from
395 liquid culture. Four genomic segments with good coverage were identified after sequencing
396 the VANA. None of these segments could be detected by RT-PCR in any other isolate but the
397 RdRp of CcPV1 in isolate Cb3.2 only.

398 A typical and complete genomic structure of *Partitiviridae* was reconstructed for CcPV1 based
399 on the structure and size of the genome as well as with sequence similarity with members of
400 the genus, the ORF of RNA1-1338 (i.e. contig1) being a polymerase and the ORF of RNA2-
401 1338 (i.e. contig2) a coat protein [57]. The ends of the 5' and 3' untranslated regions of the
402 RNA1 and 2 of CcPV1 showed strong sequence identity over more than 40 nucleotides,
403 indicating that these are two genomic segments of the same virus. The RNA1 of the CcPV1
404 isolate from *C. ramotenellum* (Cb3.2) and the RNA1 of the CcPV1 isolate from *C.*
405 *cladosporioides* (1338) shared 40/45 (88%) and 36/42 (86%) nucleotides at the 5 and 3' end
406 respectively, in line with the percentage of identity of the RNA1 coding sequence (91% aa).
407 The two genomic segments RNA1 and 2 of CcPV2 also shared highly conserved 3' and 5'-
408 UTR, allowing their unambiguous association (**Fig. 1**). Despite the lack of functional annotation
409 of ORF from RNA2 resulting from blastx analysis and CD search, determination of the protein
410 sequence of the p41 protein isolated on an acrylamide gel following purification of CcPV2 virus
411 particles by ultracentrifugation demonstrates its role as a structural protein. This result provides
412 experimental support for the assignment of a structural function to 15 closely related NCBI
413 virus sequences that were previously annotated as hypothetical proteins or annotated CP with
414 no experimental support.

415 This functional assignment extends the reach of this work to the taxonomic classification of the
416 *Gammartitivirus* genus, for which we propose to add a new clade, consisting of CcPV-2 and
417 15 hitherto unclassified viruses. This clade showed high levels of genetic diversity for both
418 RdRps and CPs, down to 19% and 9%, respectively, with the most distant members of the
419 genus. The percentage of identity for the RdRp between members of the new clade (III) and
420 the original clade (I) is below the 24% threshold set for the genus demarcation criteria, but
421 stands above this threshold when compared with viruses of clade II. The size of the CP is also
422 outside the criteria that currently defines classification in the genus *Gammartitivirus*.
423 However, the grouping of these viruses into a new genus of *Partitiviridae* would break the
424 existing monophyletic structure of the *Gammartitivirus* group. Therefore, we recommend
425 that the genus delimitation criteria for this viral family be modified to allow the incorporation of
426 these 16 isolates representing 14 to 16 new species from the additional clade within the genus

427 *Gammartitivirus*. The distinction of two clades within *Gammartitivirus* has recently been
428 proposed, and the inclusion of 16 isolates in a third clade supports and extends these recent
429 results by Wang et al. (2023).

430 The high concordance of phylogenies based on RdRp sequences on one hand and on CP
431 sequences on the other highlights two inconsistencies for UvPV and PvIaPV3. PvIaPV3 was
432 identified in a metagenomic study. In the absence of biologically available isolates and RACE-
433 PCR data to compare the complete ends of the fragments, it is not possible to verify whether
434 this inconsistency is an incorrect association of segments from two distinct viruses or cases of
435 reassortment. UvPV is an interesting case prepared from a pure culture of a *Ustilagoidea*
436 *virens* strain maintained in a collection and containing 4 viral genomic fragments. The first two
437 fragments associated by 5' end analysis correspond to a group II RdRp and CP. The third
438 fragment - unfortunately incomplete at its ends - clustered in the new clade III of
439 gammartitiviruses. Further work is required to verify whether these are two distinct viruses
440 for which an RdRp is missing, or whether this third fragment is a form of virus that is a satellite
441 of the first.

442 The characterisation of the CcPV2 genome also reveals an exceptionally long conserved
443 region spanning 69/74 nucleotides of the 3' UTR, which was almost the entire non-coding area
444 of RdRp (84 nt) and a large part of the non-coding area of CP (118 nt). This long-conserved
445 region of CcPV2 has no homology to any other virus. Highly conserved UTR of segments of
446 multipartite virus have previously been observed in viruses of different families and may extend
447 to the entire untranslated sequence [58–60]. However, in the *Partitiviridae* family, the
448 conserved motif was so far short, restricted to a few nucleotides of the untranslated ends with
449 some genus specificity [49, 61] although it sometimes extended beyond these few nucleotides
450 [62, 63].

451 The role of high conservation level of UTRs remains to be defined, but similar to the role
452 proposed for segmented viruses [64–66], it may ensure packaging and transcriptional
453 specificity to limit reassortment. Thus, this high degree of specificity of the untranslated ends
454 that distinguishes these two viral species, most likely contributes to the stability of their
455 coexistence within the same fungal strain over the last 12 years.

456 **Conclusion**

457 The two complete genomic sequences presented in this work have made it possible to extend
458 the genus *Gammartitivirus* by integrating a large set of previously unassigned sequences
459 into a new clade of this viral genus. This work has also presented a new group of capsid
460 proteins.

461

462 **Author contributions**

463 **Augustine Jaccard:** Conceptualization, Methodology, Formal analysis, Investigation, Writing
464 - Original Draft, Visualization
465 **Nathalie Dubuis:** Investigation
466 **Isabelle Kellenberger:** Investigation
467 **Justine Brodard:** Investigation
468 **Sylvain Schnee:** Writing - Review & Editing
469 **Katia Gindro:** Writing - Review & Editing
470 **Olivier Schumpp:** Conceptualization, Writing - Original Draft, Writing - Review & Editing,
471 Supervision, Project administration, Funding acquisition

472 **Acknowledgments**

473 We would like to thank François Maclot for his precious advices for VANA extraction. We are
474 grateful to Nicole Lecoultre and Emilie Michellod who helped in the fungal community
475 construction. We are also grateful to Arnaud Blouin for his careful review of the manuscript.

476 **References**

- 477 1. **Porras-Alfaro A, Bayman P.** Hidden fungi, emergent properties: Endophytes and
478 microbiomes. *Annual Review of Phytopathology* 2011;49:291–315.
- 479 2. **Belda I, Zarraonaindia I, Perisin M, Palacios A, Acedo A.** From vineyard soil to wine
480 fermentation: Microbiome approximations to explain the ‘terroir’ Concept. *Frontiers in*
481 *Microbiology*;8. Epub ahead of print May 2017. DOI: 10.3389/fmicb.2017.00821.
- 482 3. **Kashif M, Jurvansuu J, Vainio EJ, Hantula J.** Alphapartitiviruses of heterobasidion
483 wood decay fungi affect each other’s transmission and host growth. *Frontiers in Cellular*
484 *and Infection Microbiology*;9. Epub ahead of print 2019. DOI: 10.3389/fcimb.2019.00064.
- 485 4. **Knowlton N, Rohwer F.** Multispecies Microbial Mutualisms on Coral Reefs: The Host as
486 a Habitat. *The American Naturalist* 2003;162:S51–S62.
- 487 5. **Nerva L, Garcia JF, Favaretto F, Giudice G, Moffa L, et al.** The hidden world within
488 plants: metatranscriptomics unveils the complexity of wood microbiomes. *Journal of*
489 *Experimental Botany* 2022;73:2682–2697.
- 490 6. **Terhonen E, Blumenstein K, Kovalchuk A, Asiegbu FO.** Forest tree microbiomes and
491 associated fungal endophytes: Functional roles and impact on forest health. *Forests*;10.
492 Epub ahead of print January 2019. DOI: 10.3390/f10010042.
- 493 7. **Vandenkoornhuysse P, Quaiser A, Duhamel M, Le Van A, Dufresne A.** The
494 importance of the microbiome of the plant holobiont. *New Phytologist* 2015;206:1196–
495 1206.
- 496 8. **Pacifico D, Squartini A, Crucitti D, Barizza E, Lo Schiavo F, et al.** The Role of the
497 Endophytic Microbiome in the Grapevine Response to Environmental Triggers. *Frontiers*
498 *in Plant Science*;10. <https://www.frontiersin.org/article/10.3389/fpls.2019.01256> (2019,
499 accessed 4 May 2022).
- 500 9. **Nuss DL.** *Biological Control of Chestnut Blight: an Example of Virus-Mediated*
501 *Attenuation of Fungal Pathogenesis.*

- 502 10. **Rigling D, Prospero S.** Cryphonectria parasitica, the causal agent of chestnut blight:
503 invasion history, population biology and disease control. *Mol Plant Pathol* 2017;19:7–20.
- 504 11. **Zhang H, Xie J, Fu Y, Cheng J, Qu Z, et al.** A 2-kb Mycovirus Converts a Pathogenic
505 Fungus into a Beneficial Endophyte for Brassica Protection and Yield Enhancement.
506 *Molecular Plant* 2020;13:1420–1433.
- 507 12. **Al Rwahnih M, Daubert S, Úrbez-Torres JR, Cordero F, Rowhani A.** Deep
508 sequencing evidence from single grapevine plants reveals a virome dominated by
509 mycoviruses. *Arch Virol* 2011;156:397–403.
- 510 13. **Chiapello M, Rodríguez-Romero J, Ayllón MA, Turina M.** Analysis of the virome
511 associated to grapevine downy mildew lesions reveals new mycovirus lineages. *Virus*
512 *Evolution* 2020;6:veaa058.
- 513 14. **Pandey B, Naidu RA, Grove GG.** Detection and analysis of mycovirus-related RNA
514 viruses from grape powdery mildew fungus *Erysiphe necator*. *Arch Virol* 2018;163:1019–
515 1030.
- 516 15. **Bensch K, Groenewald JZ, Braun U, Dijksterhuis J, Starink M, et al.** Biodiversity in
517 the *Cladosporium herbarum* complex (Davidiellaceae, Capnodiales), with standardisation
518 of methods for *Cladosporium* taxonomy and diagnostics. *Studies in Mycology*;58. Epub
519 ahead of print 31 December 2007. DOI: 10.3114/sim.2007.58.05.
- 520 16. **Deyett E, Rolshausen PE.** Temporal Dynamics of the Sap Microbiome of Grapevine
521 Under High Pierce’s Disease Pressure. *Frontiers in Plant Science*;10.
522 <https://www.frontiersin.org/articles/10.3389/fpls.2019.01246> (2019, accessed 27
523 February 2023).
- 524 17. **Nerva L, Turina M, Zanzotto A, Gardiman M, Gaiotti F, et al.** Isolation, molecular
525 characterization and virome analysis of culturable wood fungal endophytes in esca
526 symptomatic and asymptomatic grapevine plants. *Environmental Microbiology*
527 2019;21:2886–2904.
- 528 18. **Liu D, Howell K.** Community succession of the grapevine fungal microbiome in the
529 annual growth cycle. *Environmental Microbiology* 2021;23:1842–1857.
- 530 19. **Briceño EX, Latorre BA.** Characterization of *Cladosporium* Rot in Grapevines, a
531 Problem of Growing Importance in Chile. *Plant Disease* 2008;92:1635–1642.
- 532 20. **Hofstetter V, Buyck B, Croll D, Viret O, Couloux A, et al.** What if esca disease of
533 grapevine were not a fungal disease? *Fungal Diversity* 2012;54:51–67.
- 534 21. **Pilotti M, Faggioli F, Barba M.** Characterization of italian isolates of pear vein yellows
535 virus. In: *Acta Horticulturae*. International Society for Horticultural Science (ISHS),
536 Leuven, Belgium. pp. 148–154.
- 537 22. **Mahillon M, Brodard J, Kellenberger I, Blouin AG, Schumpp O.** A novel weevil-
538 transmitted tymovirus found in mixed infection on hollyhock. *Virology Journal* 2023;20:17.
- 539 23. **Akbergenov R, Si-Ammour A, Blevins T, Amin I, Kutter C, et al.** Molecular
540 characterization of geminivirus-derived small RNAs in different plant species. *Nucleic*
541 *Acids Research* 2006;34:462–471.
- 542 24. **Candresse T, Filloux D, Muhire B, Julian C, Galzi S, et al.** Appearances can be
543 deceptive: Revealing a hidden viral infection with deep sequencing in a plant quarantine

- 544 context. *PLoS ONE*;9. Epub ahead of print July 2014. DOI:
545 10.1371/journal.pone.0102945.
- 546 25. **Filloux D, Dallot S, Delaunay A, Galzi S, Jacquot E, et al.** Metagenomics Approaches
547 Based on Virion-Associated Nucleic Acids (VANA): An Innovative Tool for Assessing
548 Without A Priori Viral Diversity of Plants. In: Lacomme C (editor). *Plant Pathology:*
549 *Techniques and Protocols*. New York, NY: Springer. pp. 249–257.
- 550 26. **Maclot FJ, Debue V, Blouin AG, Fontdevila Pareta N, Tamisier L, et al.** Identification,
551 molecular and biological characterization of two novel secovirids in wild grass species in
552 Belgium. *Virus Research* 2021;298:198397.
- 553 27. **Bankevich A, Nurk S, Antipov D, Gurevich AA, Dvorkin M, et al.** SPAdes: A New
554 Genome Assembly Algorithm and Its Applications to Single-Cell Sequencing. *Journal of*
555 *Computational Biology* 2012;19:455–477.
- 556 28. BBDuk Guide. *DOE Joint Genome Institute*. [https://jgi.doe.gov/data-and-tools/software-](https://jgi.doe.gov/data-and-tools/software-tools/bbtools/bb-tools-user-guide/bbdduk-guide/)
557 [tools/bbtools/bb-tools-user-guide/bbdduk-guide/](https://jgi.doe.gov/data-and-tools/software-tools/bbtools/bb-tools-user-guide/bbdduk-guide/) (accessed 5 June 2020).
- 558 29. **Asamizu T, Summers D, Beth Motika M, Anzola JV, Nuss DL.** *Molecular Cloning and*
559 *Characterization of the Genome of Wound Tumor Virus: A Tumor-Inducing Plant*
560 *Reovirus*. 1985.
- 561 30. **Abràmoff DMD.** Image Processing with ImageJ.
- 562 31. **Ahmed I, Li P, Zhang L, Jiang X, Bhattacharjee P, et al.** First report of a novel
563 partitivirus from the phytopathogenic fungus *Fusarium cerealis* in China. *Arch Virol*
564 2020;165:2979–2983.
- 565 32. **Nerva L, Silvestri A, Ciuffo M, Palmano S, Varese GC, et al.** Transmission of
566 *Penicillium aurantiogriseum* partiti-like virus 1 to a new fungal host (*Cryphonectria*
567 *parasitica*) confers higher resistance to salinity and reveals adaptive genomic changes.
568 *Environmental Microbiology* 2017;19:4480–4492.
- 569 33. **Edgar RC.** MUSCLE: multiple sequence alignment with high accuracy and high
570 throughput. *Nucleic Acids Res* 2004;32:1792–1797.
- 571 34. **Kalyaanamoorthy S, Minh BQ, Wong TKF, von Haeseler A, Jermin LS.** ModelFinder:
572 fast model selection for accurate phylogenetic estimates. *Nat Methods* 2017;14:587–589.
- 573 35. **Trifinopoulos J, Nguyen L-T, von Haeseler A, Minh BQ.** W-IQ-TREE: a fast online
574 phylogenetic tool for maximum likelihood analysis. *Nucleic Acids Research*
575 2016;44:W232–W235.
- 576 36. **Hoang DT, Chernomor O, von Haeseler A, Minh BQ, Vinh LS.** UFBoot2: Improving
577 the Ultrafast Bootstrap Approximation. *Molecular Biology and Evolution* 2018;35:518–
578 522.
- 579 37. **Ciccarelli FD, Doerks T, von Mering C, Creevey CJ, Snel B, et al.** Toward automatic
580 reconstruction of a highly resolved tree of life. *Science* 2006;311:1283–1287.
- 581 38. **El-Gebali S, Mistry J, Bateman A, Eddy SR, Luciani A, et al.** The Pfam protein
582 families database in 2019. *Nucleic Acids Research* 2019;47:D427–D432.

- 583 39. **Starr EP, Nuccio EE, Pett-Ridge J, Banfield JF, Firestone MK.** Metatranscriptomic
584 reconstruction reveals RNA viruses with the potential to shape carbon cycling in soil.
585 *Proceedings of the National Academy of Sciences* 2019;116:25900–25908.
- 586 40. **Vainio EJ, Chiba S, Ghabrial SA, Maiss E, Roossinck M, et al.** ICTV Virus Taxonomy
587 Profile: Partitiviridae. *J Gen Virol* 2018;99:17–18.
- 588 41. **Wang P, Yang G, Shi N, Zhao C, Hu F, et al.** A novel partitivirus orchestrates
589 conidiation, stress response, pathogenicity, and secondary metabolism of the
590 entomopathogenic fungus *Metarhizium majus*. *PLOS Pathogens* 2023;19:e1011397.
- 591 42. **Ochoa WF, Havens WM, Sinkovits RS, Nibert ML, Ghabrial SA, et al.** Partitivirus
592 structure reveals a 120-subunit, helix-rich capsid with distinctive surface arches formed
593 by quasisymmetric coat-protein dimers. *Structure* 2008;16:776–786.
- 594 43. **Chun J, Ko Y-H, Kim D-H.** Transcriptome Analysis of *Cryphonectria parasitica* Infected
595 With *Cryphonectria hypovirus 1* (CHV1) Reveals Distinct Genes Related to Fungal
596 Metabolites, Virulence, Antiviral RNA-Silencing, and Their Regulation. *Frontiers in*
597 *Microbiology*;11. <https://www.frontiersin.org/articles/10.3389/fmicb.2020.01711> (2020,
598 accessed 10 March 2023).
- 599 44. **Lemus-Minor CG, Canizares MC, Garcíá-Pedrajas MD, Pérez-Artés E.** *Fusarium*
600 *oxysporum* f. Sp. *Dianthi virus 1* accumulation is correlated with changes in virulence and
601 other phenotypic traits of its fungal host. *Phytopathology* 2018;108:957–963.
- 602 45. **Xiao X, Cheng J, Tang J, Fu Y, Jiang D, et al.** A novel partitivirus that confers
603 hypovirulence on plant pathogenic fungi. *J Virol* 2014;88:10120–10133.
- 604 46. **Ahn I-P, Lee Y-H.** A Viral Double-Stranded RNA Up Regulates the Fungal Virulence of
605 *Nectria radicola*. *MPMI* 2001;14:496–507.
- 606 47. **Bhatti MF, Jamal A, Petrou MA, Cairns TC, Bignell EM, et al.** The effects of dsRNA
607 mycoviruses on growth and murine virulence of *Aspergillus fumigatus*. *Fungal Genetics*
608 *and Biology* 2011;48:1071–1075.
- 609 48. **Filippou C, Diss RM, Daudu JO, Coutts RHA, Kotta-Loizou I.** The Polymycovirus-
610 Mediated Growth Enhancement of the Entomopathogenic Fungus *Beauveria bassiana* Is
611 Dependent on Carbon and Nitrogen Metabolism. *Frontiers in Microbiology*;12. Epub
612 ahead of print February 2021. DOI: 10.3389/fmicb.2021.606366.
- 613 49. **Gilbert KB, Holcomb EE, Aillscheid RL, Carrington JC.** Hiding in plain sight: New virus
614 genomes discovered via a systematic analysis of fungal public transcriptomes. *PLOS*
615 *ONE* 2019;14:e0219207.
- 616 50. **Kamaruzzaman M, He G, Wu M, Zhang J, Yang L, et al.** A Novel Partitivirus in the
617 Hypovirulent Isolate QT5-19 of the Plant Pathogenic Fungus *Botrytis cinerea*. *Viruses*
618 2019;11:24.
- 619 51. **Zheng L, Zhang M, Chen Q, Zhu M, Zhou E.** A novel mycovirus closely related to
620 viruses in the genus *Alphapartitivirus* confers hypovirulence in the phytopathogenic
621 fungus *Rhizoctonia solani*. *Virology* 2014;456–457:220–226.
- 622 52. **Latorre BA, Briceño EX, Torres R.** Increase in *Cladosporium* spp. populations and rot
623 of wine grapes associated with leaf removal. *Crop Protection* 2011;30:52–56.

- 624 53. **McHale MT, Roberts IN, Noble SM, Beaumont C, Whitehead MP, et al.** CfT-I: an LTR-
625 retrotransposon in *Cladosporium fulvum*, a fungal pathogen of tomato. *Molec Gen Genet*
626 1992;233:337–347.
- 627 54. **Maheshwari R, Navaraj A.** Senescence in fungi: the view from *Neurospora*. *FEMS*
628 *Microbiology Letters* 2008;280:135–143.
- 629 55. **Maas MF, Debets AJ, Zwaan BJ, others.** 17 Why Some Fungi Senesce and Others Do
630 Not. *The Evolution of Senescence in the Tree of Life* 2017;341.
- 631 56. **Vainio EJ, Jurvansuu J, Hyder R, Kashif M, Piri T, et al.** Heterobasidion Partitivirus 13
632 Mediates Severe Growth Debilitation and Major Alterations in the Gene Expression of a
633 Fungal Forest Pathogen. Epub ahead of print 2018. DOI: 10.1128/JVI.
- 634 57. **Bozarth RF, Wood HA, Mandelbrot A.** The *Penicillium stoloniferum* virus complex: Two
635 similar double-stranded RNA virus-like particles in a single cell. *Virology* 1971;45:516–
636 523.
- 637 58. **Chiba S, Salaipeth L, Lin Y-H, Sasaki A, Kanematsu S, et al.** A Novel Bipartite
638 Double-Stranded RNA Mycovirus from the White Root Rot Fungus *Rosellinia necatrix*:
639 Molecular and Biological Characterization, Taxonomic Considerations, and Potential for
640 Biological Control. *Journal of Virology* 2009;83:12801–12812.
- 641 59. **Wu M, Jin F, Zhang J, Yang L, Jiang D, et al.** Characterization of a Novel Bipartite
642 Double-Stranded RNA Mycovirus Conferring Hypovirulence in the Phytopathogenic
643 Fungus *Botrytis porri*. *Journal of Virology* 2012;86:6605–6619.
- 644 60. **Liu L, Wang Q, Cheng J, Fu Y, Jiang D, et al.** Molecular characterization of a bipartite
645 double-stranded RNA virus and its satellite-like RNA co-infecting the phytopathogenic
646 fungus *Sclerotinia sclerotiorum*. *Frontiers in Microbiology*;6.
647 <https://www.frontiersin.org/articles/10.3389/fmicb.2015.00406> (2015, accessed 5 June
648 2023).
- 649 61. **Nibert ML, Ghabrial SA, Maiss E, Lesker T, Vainio EJ, et al.** Taxonomic
650 reorganization of family Partitiviridae and other recent progress in partitivirus research.
651 *Virus Research* 2014;188:128–141.
- 652 62. **Wang Y, Zhao H, Cao J, Yin X, Guo Y, et al.** Characterization of a Novel Mycovirus
653 from the Phytopathogenic Fungus *Botryosphaeria dothidea*. *Viruses* 2022;14:331.
- 654 63. **Hamim I, Urayama S, Netsu O, Tanaka A, Arie T, et al.** Discovery, Genomic Sequence
655 Characterization and Phylogenetic Analysis of Novel RNA Viruses in the Turfgrass
656 Pathogenic *Colletotrichum* spp. in Japan. *Viruses* 2022;14:2572.
- 657 64. **Robertson JS.** 5' and 3' terminal nucleotide sequences of the RNA genome segments of
658 influenza virus. *Nucleic Acids Research* 1979;6:3745–3758.
- 659 65. **McDonald SM, Nelson MI, Turner PE, Patton JT.** Reassortment in segmented RNA
660 viruses: mechanisms and outcomes. *Nat Rev Microbiol* 2016;14:448–460.
- 661 66. **Gao Q, Palese P.** Rewiring the RNAs of influenza virus to prevent reassortment. *Proc*
662 *Natl Acad Sci USA* 2009;106:15891–15896.

663
664